

Random matrix models for chiral and diquark condensation

Benoît Vanderheyden

*Department of Electrical Engineering and Computer Science,
Montefiore Bât. B-28, University of Liège,
B-4000 Liège (Sart-Tilman), Belgium*

A. D. Jackson

*The Niels Bohr Institute, Blegdamsvej 17, DK-2100 Copenhagen Ø, Denmark
(Dated: March 2, 2005)*

We consider random matrix models for the thermodynamic competition between chiral symmetry breaking and diquark condensation in QCD at finite temperature and finite baryon density. The models produce mean field phase diagrams whose topology depends solely on the global symmetries of the theory. We discuss the block structure of the interactions that is imposed by chiral, spin, and color degrees of freedom and comment on the treatment of density and temperature effects. Extension of the coupling parameters to a larger class of theories allows us to investigate the robustness of the phase topology with respect to variations in the dynamics of the interactions. We briefly study the phase structure as a function of coupling parameters and the number of colors.

PACS numbers: 11.30. Fs, 11.30. Qc, 11.30. Rd, 12.38. Aw

I. INTRODUCTION

Some thirty years ago, it was observed that dense and cold quark matter might exhibit Cooper pairing as a result of an attractive quark-quark interaction in the color antitriplet channel [1]. More recent models, based on non-perturbative effective interactions or on diagrammatic calculations of single-gluon exchange interactions, indicate that a color superconducting phase might develop pairing gaps as large as $\Delta \sim 100$ MeV for quark chemical potentials on the order of 300 MeV [2]. This interesting possibility has direct consequences on the physics of dense stars and is certainly important for the determination of the phase diagram of nuclear matter under extreme (ultrarelativistic) conditions [3, 4].

Different order parameters have been proposed in the literature and studied as a function of, e.g., the quark masses, the number of flavors and colors, the quark chemical potentials, and temperature [3, 4]. In the limit of QCD with two flavors of light quarks (the 2SC limit), the order parameter has the form

$$\langle \psi_{f\alpha\sigma}(p) \psi_{g\beta\sigma'}(-p) \rangle = \Phi(p^2) \varepsilon_{fg} \varepsilon_{\alpha\beta 3} \varepsilon_{\sigma\sigma'}, \quad (1)$$

where p is a four-momentum and where we have displayed the flavor (f, g), color (α, β), and spin (σ, σ') indices. The tensors ε ensures that the condensate is antisymmetric in flavor, color, and spin. Color is broken from $SU(3)$ to $SU(2)$, but the flavor symmetry $SU(2)_L \times SU(2)_R$ and the baryon symmetry $U(1)_B$ remain intact. In the other limit of three degenerate flavors of light quarks, the favored order parameter exhibits a coupling between color and flavor rotations (called color-flavor locking or CFL) and has the approximate form [3]

$$\langle \psi_{f\alpha\sigma}(p) \psi_{g\beta\sigma'}(-p) \rangle = \Phi(p^2) \varepsilon_{fgA} \varepsilon_{\alpha\beta A} \varepsilon_{\sigma\sigma'}. \quad (2)$$

Color, flavor, and baryon symmetries are now broken down to $SU(3)_{\text{color}+L+R} \times Z_2$. Since both $SU(3)_L$ and $SU(3)_R$ are locked to $SU(3)_{\text{color}}$, the CFL condensate also breaks chiral symmetry.

Following Ref. [4], the conjectured phase diagram for QCD with three flavors and realistic quark masses is given in Fig. 1. At asymptotically high densities, the scale is set by the quark chemical potential, μ . For $\mu \gg m_s$ (m_s is the strange quark mass), the more symmetric CFL phase is favored. As μ decreases, the increasing difference between u - (or d -) and s -quark Fermi momenta weakens $\langle us \rangle$ and $\langle ds \rangle$ condensates and eventually leads to a transition to the 2SC phase [5], possibly via a so-called LOFF phase characterized by a spatially varying gap [6].

Most of these results have not been confirmed by lattice simulations, which are difficult to perform and interpret for QCD with three colors at finite baryon densities. The difficulty resides in the fact that the fermion determinant in the partition function is complex for non-zero μ , and sampling weights are no longer positive definite. This difficult problem represents a significant barrier to understanding the phase structure of QCD in lattice simulations.

Random matrix theory offers models that are capable of distinguishing those physical properties that are determined by global symmetries from those that depend on the detailed dynamics of the interactions. The random matrix Hamiltonian mimics the true interactions by adopting a block structure that is solely determined by the global

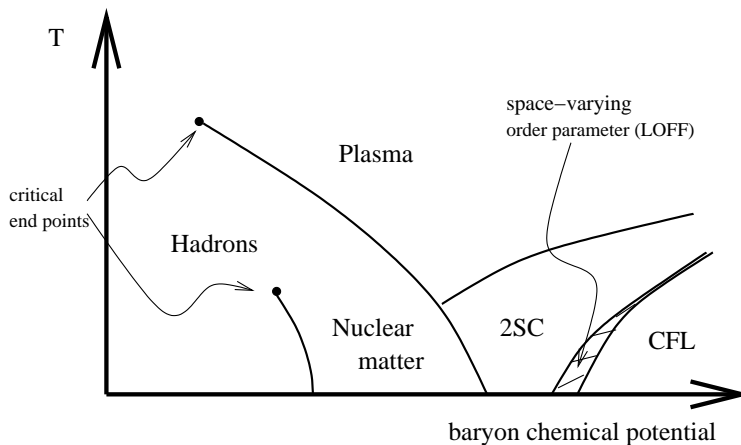


FIG. 1: Sketch of the phase diagram for three flavor QCD with realistic quark masses. After Ref. [4].

symmetries under consideration. The matrix elements are drawn on a random distribution, usually a Gaussian distribution, so that the model can be solved exactly. Such an approach leads to universal results that can be studied at two different levels. At the microscopic level, the statistical properties of the lowest eigenvalues of the Dirac operator are determined by the spontaneous breaking of chiral symmetry, as indicated for example by the universality of the spectral density near zero virtuality and related sum rules [7, 8, 9, 10]. At the macroscopic level, many of the properties of the phase diagram (such as its topology and the presence of given critical lines or points) are independent of the detailed form of the interactions and are thus symmetry protected. The random matrix approach treats low-lying fermion excitations and, in its usual form, neglects their momentum and kinetic energy. The resulting phase diagram is mean-field. Near critical regions, it produces results similar to those obtained in a Landau-Ginzburg approach [11, 12]. In general, random matrix models provide a useful tool for studying systems with non-trivial phase diagrams.

This talk focuses on random matrix models that implement coexisting chiral and color symmetries in QCD with two light degenerate flavors (2SC). These models are extensions of the chiral random matrix models, which we introduce in Sec. II. We present the construction of the color and spin block structure of the interactions in Sec. III. The phase diagram is discussed in Sec. IV. This talk is a summary of previous work on the question, see Refs. [13, 14, 15].

II. CHIRAL RANDOM MATRIX MODELS

We first consider chiral symmetry alone and turn to chiral random matrix models [16, 17]. For QCD in the sector of zero topological charge with N_f flavors and zero chemical potential, the partition function is given as

$$Z = \int DW \prod_{i=1}^{N_f} D\psi_i^* D\psi_i \exp \left[i \sum_{i=1}^{N_f} \psi_i^* \mathcal{D} \psi_i \right] \exp \left(- \frac{n\beta\Sigma^2}{2} \text{Tr}[WW^\dagger] \right), \quad (3)$$

where W is an $n \times n$ matrix which models the interactions. Its elements are drawn on a Gaussian distribution of mean zero and inverse variance Σ . Here, n is a measure of the number of low-lying degrees of freedom and is to be taken to infinity at the end of the calculations (i.e., in the thermodynamic limit). In the chiral limit, $m = 0$, the Dirac operator, \mathcal{D} , has a block structure imposed by the chiral symmetry of QCD, $\{D, \gamma_5\} = 0$. In the basis of the eigenstates of γ_5 , this leads to the block structure

$$\mathcal{D} = \begin{pmatrix} 0 & iW \\ iW^\dagger & 0 \end{pmatrix}. \quad (4)$$

For random matrix models of QCD with $SU(3)$ and fermions in the fundamental representation, W is complex. This choice corresponds to the chiral unitary ensemble, which is characterized by a Dyson index $\beta = 2$. The QCD Dirac operator in $SU(2)$ with fermions in the fundamental representation satisfies an additional anti-unitary symmetry,

$$[C(\sigma_2)_{\text{color}} K, i\mathcal{D}] = 0, \quad (5)$$

with $(C(\sigma_2)_{\text{color}}K)^2 = 1$. (C is the charge conjugation operator, σ_2 is the antisymmetric color matrix, and K is the complex conjugation operator.) This implies that it is possible to find a particular basis of states in which $i\mathcal{D}$ is real. Accordingly, W is chosen real in chiral random matrix models for $SU(2)$, and this leads to the chiral orthogonal ensemble with an index $\beta = 1$ [17]. For fermions in the adjoint representation of the gauge group and any number of colors, the Dirac operator obeys the anti-unitary symmetry $C^{-1}K$ with $(C^{-1}K)^2 = -1$. This leads to the symplectic chiral ensemble with $\beta = 4$ and quaternion real matrix elements [10, 17]. We will not consider this ensemble further in this talk.

The essential difference among the ensembles lies in the number of independent random variables that are allowed per matrix element. (I.e., A complex number has two degrees of freedom; a real number has only one.) This difference is important in determining the statistical properties of the Dirac operator and, in turn, affects the phase diagram.

III. RANDOM MATRIX MODELS WITH AN EXPANDED BLOCK STRUCTURE

In order to study the competition between chiral, $\langle \bar{q}q \rangle$, and diquark, $\langle q^T q \rangle$, condensates, we introduce an explicit dependence in the spin and color quantum numbers appearing in the 2SC order parameter of Eq. (1). We are thus lead to a Dirac operator with the chiral block structure of Eq. (4), where W now has the following expanded color and spin sub-block structure:

$$W = \sum_{\mu=0}^3 \sum_{a=1}^{N_c^2-1} \lambda_a \otimes \sigma_\mu \otimes A_{\mu a}. \quad (6)$$

Here, the deterministic matrices represent spin and color degrees of freedom: $\sigma_\mu = (1, i\vec{\sigma})$ with $\vec{\sigma}$ the Pauli matrices, whereas λ_a are color matrices (Gell-Mann matrices for $N_c = 3$). The random matrices, $A_{\mu a}$, are $N \times N$ and represent gluon fields. They are chosen real. Their elements are drawn on a Gaussian distribution with an inverse variance that is independent of μ and a in order to respect the Lorentz and $SU(N_c)$ invariance in the vacuum.

Including a quark chemical potential, μ , a quark mass, m , and a temperature dependence, the partition function is now written as

$$Z = \int D\psi_1^\dagger D\psi_1 D\psi_2^* D\psi_2^T \left\{ \prod_{\mu a} DA_{\mu a} \right\} \exp \left(-2N\Sigma^2 \sum_{\mu a} \text{Tr}[A_{\mu a} A_{\mu a}^T] \right) \\ \times \exp \left[i \begin{pmatrix} \psi_1^\dagger \\ \psi_2^T \end{pmatrix}^T \begin{pmatrix} i\mathcal{D} + im + C_+ & 0 \\ 0 & -i\mathcal{D}^T - im - C_-^T \end{pmatrix} \begin{pmatrix} \psi_1 \\ \psi_2^* \end{pmatrix} \right], \quad (7)$$

where the dependence on the external parameters is given by $C_\pm = (\mp\sigma_3\pi T + i\mu)\gamma_4$ with

$$\gamma_4 = \begin{pmatrix} 0 & 1 \\ 1 & 0 \end{pmatrix}. \quad (8)$$

Note that we have used a Gorkov representation and have transposed the flavor-2 fields so that the diquark condensate appears as an off-diagonal component of the inverse Dirac operator.

Several comments are in order regarding the μ and T dependences. The μ dependence mimics the $\mu\psi^\dagger\gamma_4\psi$ term in the Euclidean QCD Lagrangian [11]. The T dependence is based on two assumptions. First, temperature is introduced via a sum over the fermion Matsubara frequencies, $\omega_n = in\pi T$ with n odd. As random matrix theory only treats low-lying degrees of freedom, much of the critical physics can be captured if one restricts the frequency sum to its two lowest terms [18], hence the two-dimensional form $\sigma_3\pi T = \text{diag}(\pi T, -\pi T)$. The second assumption comes from the physical observation that the diquark order parameter in Eq. (1) couples fields of opposite four-momenta. We explicitly impose this coupling in Eq. (7) by taking opposite Matsubara frequencies for each flavor. Different temperature dependences have been proposed in closely related random matrix models [19, 20]; we discuss their relationship to the present models in [21].

IV. PHASE DIAGRAMS

The partition function can be evaluated following a classical method. An integration over $A_{\mu a}$ produces a four-fermion interaction which can be Fierz-transformed to obtain the chiral and diquark channel terms. The resulting

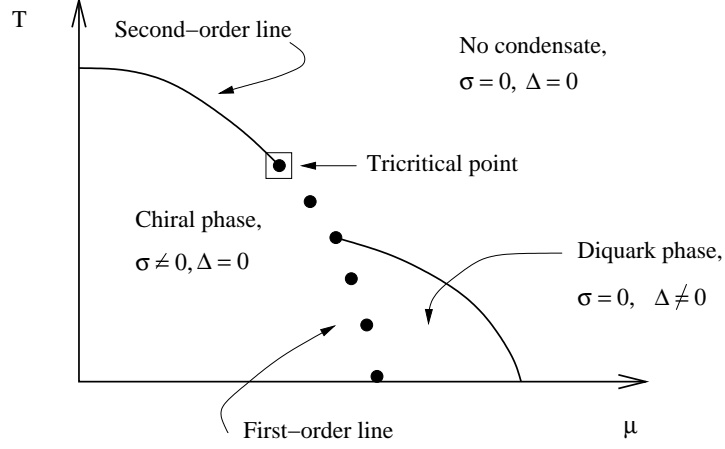


FIG. 2: Phase diagram in the random matrix model for QCD with three colors and massless quarks.

four-fermion potential can be expressed as a fermion field bilinear via a Hubbard-Stratonovitch transformation. These successive steps yield [13]

$$Z \sim \int d\sigma d\Delta e^{-4N\Omega(\sigma,\Delta)}, \quad (9)$$

where the thermodynamical potential, $\Omega(\sigma, \Delta)$, is given as

$$\Omega(\sigma, \Delta) = A\Delta^2 + B\sigma^2 - \frac{N_c - 2}{2} \sum_{\pm} \log((\sigma + m \pm \mu)^2 + \pi^2 T^2) - \sum_{\pm} \log((\sigma + m \pm \mu)^2 + \pi^2 T^2 + \Delta^2). \quad (10)$$

Here, Δ is the auxiliary field associated with the diquark channel (with condensates $\langle \psi_{2R}^T (i\sigma_2)_{\text{spin}} \lambda_2 \psi_{1R} \rangle = \langle \psi_{2L}^T (i\sigma_2)_{\text{spin}} \lambda_2 \psi_{1L} \rangle$), while σ is related to the chiral channel (with condensates $\langle \psi_1^\dagger \psi_1 \rangle = -\langle \psi_2^T \psi_2^* \rangle$). The partition function can be treated exactly in the thermodynamic limit $N \rightarrow \infty$ by a saddle point method. The equilibrium values of the field then satisfy the two gap equations

$$\frac{\partial \Omega}{\partial \sigma} = 0, \quad (11)$$

$$\frac{\partial \Omega}{\partial \Delta} = 0, \quad (12)$$

which constitute a system of polynomial equations that can be solved analytically or numerically.

The form of the potential in Eq. (10) has a straightforward interpretation. The quadratic terms correspond to the energy cost for having constant auxiliary fields. The logarithmic terms are to be related to the single quasiparticle spectrum in a given set of fields σ and Δ . Keeping in mind that the fermion four-momenta are neglected, these energies are given as $\varepsilon = ((\sigma + m \mp \mu)^2 + \Delta^2)^{1/2}$ for the two pairing colors (with the \mp sign standing for either quark or antiquark excitations). For the $N_c - 2$ unpaired colors, $\varepsilon = |\sigma + m \mp \mu|$.

We now turn to a chiral symmetric theory with $m = 0$. Note that, because it is possible to rescale all fields and external parameters by a constant, the topology of the phase diagram depends only on the ratio B/A . This is in fact a ratio of the Fierz constants in the chiral and diquark channel, and it measures the relative importance of the two symmetries. For example, small ratios are obtained with $A \gg B$; the energy cost of $A\Delta^2$ then prohibits diquark condensation. Similarly, large ratios B/A disfavor chiral symmetry breaking. For $N_c = 3$, the interactions in Eq. (6) lead to a ratio $B/A = 3/4$, which corresponds to the phase diagram of Fig. 2. One observes a low-density chiral broken symmetry phase separated from a higher density diquark phase by a first-order line. As the temperature is raised, the diquark phase makes a transition to the chiral symmetric phase across a second-order line. The transition from broken to restored chiral symmetry is second-order at low densities and first-order at intermediate densities. The two lines are separated by a tricritical point, in the vicinity of which the thermodynamical potential reduces to a ϕ^6 theory [11, 13].

It is interesting to ask how the phase structure evolves if one changes the channel couplings A and B from the values representative of QCD. To this end, we have considered Hermitean Dirac $i\mathcal{D}$ operators spanning an exhaustive set of combinations of helicity, spin, and color block structures. Remarkably, this set produces ratios B/A in the *bounded*

range $[0, N_c/2]$. This result differs from what would have been obtained in a pure Landau-Ginsburg approach, where there is no *a priori* knowledge of existing constraints among the coefficients of the effective thermodynamical potential. Here, however, having started at a more microscopic level, we are capable of discovering possible bounds on the coupling ratios. Each ratio corresponds to a separate phase structure. The major conclusions resulting from the study of phase diagrams for ratios in the allowed range are as follows:

- there is only a finite number of different topologies. As B/A is varied continuously, the evolution from one topology to another is marked by the emergence or the vanishing of new critical points or lines;
- it takes moderate — but finite — alterations of the theory to depart from the topology of Fig. 2. In that sense, the phase structure of Fig. 2 is protected by symmetry.

V. DISCUSSION

A. Comparison with a microscopic theory

In order to appreciate the approximations involved in the formulation of the random matrix model, consider the gap equation in the limit $\sigma = 0$,

$$\frac{\partial \Omega}{\partial \Delta} = 0 \Rightarrow A \Delta = \frac{2\Delta}{\Delta^2 + \mu^2 + \pi^2 T^2}, \quad (13)$$

and compare with that obtained in a microscopic mean-field theory such as that of Ref. [22], based on an effective interaction modeled by that induced by instantons. Approximately, we find

$$\Delta \simeq G \int \frac{d^4 p}{(2\pi)^4} \left(\frac{2\Delta}{\Delta^2 + (p - \mu)^2 + p_4^2} + \frac{2\Delta}{\Delta^2 + (p + \mu)^2 + p_4^2} \right), \quad (14)$$

where we have dropped the form factors needed for the convergence of the integral. It is also implied that the integral over p_4 is a sum over Matsubara frequencies, $p_4 = n\pi T$ with n odd.

Because we have neglected the fermion four-momenta, the gap equation in the random matrix approach does not contain an integral. This has two consequences. First, the right term in Eq. (13) does not exhibit the logarithmic divergence observed in Eq. (14) for $p \simeq \mu$ and $\Delta = 0$. This divergence arises for values of p near the Fermi momentum in the limit $\Delta \rightarrow 0$ and implies that a non-zero Δ must develop at all μ . In contrast, the diquark phase in Fig. 2 does not exist for asymptotically high values of μ . The random matrix interactions saturate in the diquark channel for μ larger than $\sim \Sigma$. The second consequence of the absence of a momentum integral is that the gap, Δ , evolves monotonically as a function of μ in contrast to results from a microscopic approach, see Refs. [22, 23].

These discrepancies should not be considered as weaknesses of the random matrix approach. In the first case, Δ vanishes in a region where microscopic theories tend to produce small gaps which probably do not survive fluctuations beyond mean field. What random matrix cannot reproduce, however, is the $\Delta \sim e^{-1/g}$ behavior as a function of the QCD coupling constant, g . This behavior is due to the magnetic gluon interactions [24]. The random matrix approach is also unable to reproduce the unbounded increase of Δ at asymptotically high μ , which is related to the running of g [25]. Both these features are predicted from diagrammatic theory and are related to particular dynamic processes. The second observed difference, the variation of gaps at moderate values of μ , arises from the detailed dynamics of the interactions and depends on the choice of the regulating form factors. This behavior is not dictated by symmetry, and it is thus no surprise that it is not revealed by the random matrix approach.

B. QCD with two colors

In the limit of $N_c = 2$, the gauge group is pseudoreal, and quark and antiquark states transform similarly under global color rotations. They can be combined into spinors which obey an extended flavor symmetry $SU(2N_f)$ for which $\langle \bar{q}q \rangle$ mesons and $\langle qq \rangle$ baryons belong to the same multiplets. The random matrix model (with $N_f = 2$) reproduces this extended symmetry in the vacuum and its breaking pattern as a function of μ , T , and m . In the vacuum and in the chiral limit, the thermodynamic potential depends on the condensation fields through the combination $\sigma^2 + \Delta^2$. The extended $SU(4)$ symmetry is here apparent since a state with $(\sigma, \Delta) = (\Sigma, 0)$ is indistinguishable from its rotated version with $(\sigma, \Delta) = (0, \Sigma)$. For $m > 0$ and low temperature, the phase $(\Sigma, 0)$ undergoes a second order phase transition to a diquark phase at $\mu_c \simeq m_\pi/2$ where $m_\pi \sim (m\Sigma)^{1/2}$ is the pion mass [14]. Many results of the random matrix approach agree with chiral perturbation theory in this case [26].

C. Two more questions

The random matrix model is a theory of low-lying modes. We argued earlier that restricting the sum over Matsubara frequencies leads to a model which nicely captures the critical physics. The neglect of high-energy modes leads however to unphysical results, such as a negative baryon density and a variation of the chiral field as a function μ , both in a theory with $N_c = 2$ and in the region $\mu < m_\pi/2$. We have shown that the inclusion of appropriate high-energy terms (which should not describe the critical physics), either in the form of correction terms or as a sum over all Matsubara frequencies, fixes these anomalies while leaving the topology of the phase diagram intact [14].

Another question is whether the interactions in Eq. (6) preserves the statistical properties of the eigenvalues of the Dirac operator that are expected from chiral symmetry alone. These properties should follow the predictions of the chiral unitary ensemble for QCD with three colors and those of the chiral orthogonal ensemble for QCD with two colors. This question is related to the number of random degrees of freedom allowed for the matrix elements. We have shown that, even if the interaction matrices are complex for both $N_c = 3$ and $N_c = 2$, the deterministic spin and color dependences lead to the properties that are expected for the spectrum of the Dirac operator [15].

VI. SUMMARY

We have considered random matrix models of QCD with two flavors that are capable of developing chiral and diquark condensation. We have studied the symmetry breaking patterns as a function of temperature and quark chemical potential. The phase diagrams can be established exactly from an analytical evaluation of the partition function. The resulting thermodynamical potential has a straightforward interpretation in terms of elementary excitations. Upon arbitrary variations of the coupling constants in the two condensation channels, the phase structure evolves continuously but can only adopt a fixed set of topologies.

This study shows that random matrix theory provides useful tools for studying systems with non-trivial phase diagrams and for distinguishing those properties that are protected by symmetry.

-
- [1] B. Barrois, Nucl. Phys. **B129** (1977) 390; D. Bailin and A. Love, Phys. Rept. **107** (1984) 325.
 - [2] M. Alford, K. Rajagopal, and F. Wilczek, Phys. Lett. B **422** (1998) 247; R. Rapp, T. Schäfer, E. V. Shuryak, and M. Velkovsky, Phys. Rev. Lett. **81** (1998) 53.
 - [3] K. Rajagopal and F. Wilczek, in B. L. Ioffe Festschrift, *At the Frontier of Particle Physics/Handbook of QCD*, M. Shifman ed., (World Scientific 2001); M. Alford, Ann. Rev. Nucl. Part. Sci. **51** (2001) 131; H.-c. Ren, hep-ph/0404074.
 - [4] T. Schäfer, hep-ph/0304281.
 - [5] M. Alford, J. Berges, and K. Rajagopal, Nucl. Phys. **558** (1999) 219; T. Schäfer and F. Wilczek, Phys. Rev. D **60** (1999) 074014.
 - [6] M. Alford, J. Bowers, and K. Rajagopal, Phys. Rev. D **63** (2001) 074016.
 - [7] J. J. M. Verbaarschot and I. Zahed, Phys. Rev. Lett. **70** (1993) 3852.
 - [8] J. J. M. Verbaarschot, Nucl. Phys. **B427** (1994) 534.
 - [9] J. J. M. Verbaarschot, Phys. Lett. **B329** (1994) 351.
 - [10] See for instance the review by J. J. M. Verbaarschot and T. Wettig, Ann. Rev. Nucl. Part. Sci. **50** (2000) 343.
 - [11] M. A. Halasz, A. D. Jackson, R. E. Shrock, M. A. Stephanov, and J. J. M. Verbaarschot, Phys. Rev. D **58** (1998) 096007.
 - [12] K. Iida and G. Baym, Phys. Rev. D **63** (2001) 074018; Phys. Rev. D **66** (2002) 059903(E); Phys. Rev. D **66** (2002) 014015; I. Giannakis and H.-C. Ren, Nucl. Phys. **B669** (2003) 462.
 - [13] B. Vanderheyden and A. D. Jackson, Phys. Rev. D **61** (2000) 076004; Phys. Rev. D **62** (2000) 094010.
 - [14] B. Vanderheyden and A. D. Jackson, Phys. Rev. D **64** (2001) 074016.
 - [15] B. Vanderheyden and A. D. Jackson, Phys. Rev. D **67** (2003) 085016.
 - [16] E. V. Shuryak and J. J. M. Verbaarschot, Nucl. Phys. **A560** (1993) 306.
 - [17] J. J. M. Verbaarschot, Phys. Rev. Lett. **72** (1994) 2531.
 - [18] A. D. Jackson and J. J. M. Verbaarschot, Phys. Rev. D **53** (1996) 7223.
 - [19] B. Klein, D. Toublan, and J. J. M. Verbaarschot, Phys. Rev. D **68** (2003) 014009.
 - [20] B. Klein, D. Toublan, and J. J. M. Verbaarschot, [arXiv:hep-ph/0405180].
 - [21] B. Vanderheyden and A. D. Jackson (to be published).
 - [22] J. Berges and K. Rajagopal, Nucl. Phys. **B538** (1999) 215.
 - [23] See also the contribution by D. Blaschke, this issue.
 - [24] D. T. Son, Phys. Rev. D **59** (1999) 094019.
 - [25] T. Schäfer and F. Wilczek, Phys. Rev. D **60** (1999) 114033.
 - [26] J. B. Kogut, M. A. Stephanov, D. Toublan, J. J. M. Verbaarschot, and A. Zhitnitsky, Nucl. Phys. **B582** (2000) 477.